Mon. Not. R. astr. Soc. (1992) **258**, 811–818

A simple approach to the evolution of twisted accretion discs

J. E. Pringle ★ †

Space Telescope Science Institute,‡ 3700 San Martin Drive, Baltimore, MD 21218, USA

Accepted 1992 April 27. Received 1992 April 13

ABSTRACT

A simple set of equations is introduced which governs the time evolution of a twisted accretion disc. The time evolution is governed by two 'viscosities', one governing shear within the plane of the disc and the other governing shear perpendicular to the disc (brought about by non-planarity of the disc). It is shown that these equations can be put in numerical difference form so that angular momentum is locally conserved. Numerical simulations are given for two simple cases, the evolution of a simple twist in a steady Keplerian accretion disc, and the effect of precession about an axis which is not aligned with the disc on the inner regions of the disc (the Bardeen–Petterson effect). It is emphasized that the methods presented here can be applied to more general rotation laws, and precession rates – for example, warped gaseous discs in galactic potentials.

Key words: accretion, accretion discs – celestial mechanics, stellar dynamics.

1 INTRODUCTION

The behaviour of non-planar (twisted or tilted) accretion discs subject to external torques has been discussed in the stellar context by a number of authors (Bardeen & Petterson 1975; Petterson 1977, 1978; Hatchett, Begelman & Sarazin 1981; Papaloizou & Pringle 1983). In the last-named paper, Papaloizou & Pringle (1983) pointed out that the twist evolution equations derived by the previous authors were incorrect, because they did not conserve angular momentum. Papaloizou & Pringle then went on to derive the twist evolution equation for the case of a slightly tilted disc, in the regime when the disc twist angle, i, is much less than the disc opening angle, H/R (here H is disc semithickness and R is disc radius). In this regime and for large enough viscosity, the resonant flows induced in the disc by the tilt are formally small enough to ensure the validity of linear theory. However, many cases of astrophysical interest fall in the regime where the Papaloizou–Pringle analysis does not apply, and, for example, where the resonantly induced shear flows calculated by Papaloizou & Pringle would be unstable (Papaloizou & Pringle 1983; Kumar & Pringle 1985; Coleman & Kumar 1992). This is particularly true of warped gaseous discs in the galactic context, where often the warp itself is severe, and also the axis of precession induced by the galactic potential is at a large angle to the axis of symmetry of the disc (Kahn & Woltjer 1959; Gunn 1979; Athanassoula & Bosma 1985). In this case, a number of authors have used numerical simulations (usually particle-based) to follow the evolution of a ring or disc of gas orbiting within a galaxy (Tubbs 1980; Habe & Ikeuchi 1985; Varnas 1986, 1990; Katz & Rix 1992). The problem with such calculations is that the evolution needs to be followed on the dynamical (orbital) time-scale, whereas the time-scales of interest (precession and viscous) can be very much longer. To circumvent this problem of mismatched time-scales, Steiman-Cameron & Durisen (1988) developed a method for treating each annulus in the disc as being in centrifugal balance (thus obviating the need to consider the dynamical time-scale) and then calculating the mutual interactions of such annuli, as well as their response to external torques. Such an approach is exactly analogous to the one employed in the case of stellar discs (Petterson 1977, 1978; Hatchett, Begelman & Sarazin 1981). Note, however, that such an approach does exclude consideration of resonant interactions (e.g., Borderies, Goldreich & Tremaine 1984; Lubow 1992). Unfortunately, the mutual interactions between neighbouring annuli in the numerical implementation given by Steiman-Cameron & Durisen do not appear to obey Newton's Third Law, implying in effect that the method does not locally (or globally) conserve angular momentum.

In this paper we derive, in Section 2, a set of analytic equations which govern disc tilt using the simplified assumption described above to eliminate the dynamical time-scale. Mutual viscous interactions between neighbouring annuli fall

★ On leave from the Institute of Astronomy, Cambridge.
† Affiliated with the Astrophysics Division, Space Science Department of ESA.
‡ Operated by AURA, Inc., under contract with NASA.

into two types – those concerned with shear within the disc plane due to differential rotation, to which we assign a viscosity ν_1, and those concerned with shear perpendicular to the disc plane due to disc twist, to which we assign a viscosity ν_2. We discuss below (Section 5) why it is not evident that the two coefficients of viscosity should be the same. The equations are derived in such a form that it is explicitly obvious that angular momentum is locally conserved. In Section 3 we describe how these analytic equations can be transformed into a numerical scheme which maintains the benefit of local conservation of angular momentum to machine accuracy. In Section 4, by way of illustration, we apply the numerical scheme to a couple of simple cases. We discuss the results in Section 5.

2 DERIVATION OF THE EQUATIONS

We consider a disc such that, at each radius R from the centre, the material is centrifugally supported in primarily circular orbits with angular velocity $\Omega(R)$. Note that R is a purely radial coordinate and not the cylindrical radius. At each radius, the disc has a unit tilt vector $\boldsymbol{l}(R, t)$, defined such that, to first order, the annulus of material contained between $R-\frac{1}{2}\Delta R$ and $R+\frac{1}{2}\Delta R$ has angular momentum $\Delta \boldsymbol{L}=2\pi\Sigma\cdot\Delta R\cdot R^2\Omega\,\boldsymbol{l}$, where $\Sigma(R, t)$ is the surface density of the disc. We assume the disc at each radius to be thin in the direction of $\boldsymbol{l}$. For such a disc, the basic conservation equations are derived by Papaloizou & Pringle (1983). The mass conservation equation is

$$\frac{\partial\Sigma}{\partial t}+\frac{1}{R}\frac{\partial}{\partial R}(R\Sigma V_R)=0, \tag{2.1}$$

where $V_R(R, t)$ is the radial velocity in the disc, and the angular momentum conservation equation is

$$\frac{\partial}{\partial t}(\Sigma R^2\Omega\,\boldsymbol{l})+\frac{1}{R}\frac{\partial}{\partial R}(\Sigma V_R R^3\Omega\,\boldsymbol{l})=\frac{1}{R}\frac{\partial}{\partial R}(\nu_1\Sigma R^3\Omega'\boldsymbol{l}) \tag{2.2}$$

$$+\frac{1}{R}\frac{\partial}{\partial R}\left(\frac{1}{2}\nu_2\Sigma R^3\Omega\frac{\partial\boldsymbol{l}}{\partial R}\right).$$

Here $\Omega'=\mathrm{d}\Omega/\mathrm{d}R$, ν_1 is the viscosity corresponding to the azimuthal shear, and ν_2 the viscosity corresponding to vertical shear. Thus ν_1 is the shear viscosity normally associated with accretion discs, whereas ν_2 is associated with straightening out the out-of-plane motions (i.e., the twist).

Papaloizou & Pringle (1983) went on to analyse these equations in the case of small tilt, but here we wish to retain full generality. Simple manipulation of these two equations yields an equation for the radial velocity:

$$V_R=\frac{(\partial/\partial R)(\nu_1\Sigma R^3\Omega')-\frac{1}{2}\nu_2\Sigma R^3\Omega|\partial\boldsymbol{l}/\partial R|^2}{R\Sigma(\partial/\partial R)(R^2\Omega)} \tag{2.3}$$

We then substitute this into equation (2.1) to obtain the equation describing the time evolution of surface density:

$$\frac{\partial\Sigma}{\partial t}=\frac{1}{R}\frac{\partial}{\partial R}\left\{\frac{(\partial/\partial R)[\nu_1\Sigma R^3(-\Omega')]}{(\partial/\partial R)(R^2\Omega)}\right\} \tag{2.4}$$

$$+\frac{1}{R}\frac{\partial}{\partial R}\left[\frac{\frac{1}{2}\nu_2\Sigma R^3\Omega|\partial\boldsymbol{l}/\partial R|^2}{(\partial/\partial R)(R^2\Omega)}\right].$$

The physical meaning of the two terms on the right-hand side is fairly clear. When the disc is flat ($\partial\boldsymbol{l}/\partial R=0$), the equation reduces to the standard accretion disc evolution equation (e.g., Pringle 1981), and thus the first term on the right-hand side is a diffusive term governed by ν_1. The second term on the right-hand side is, mathematically speaking, an advective term with inwards flow velocity proportional to $\nu_2|\partial\boldsymbol{l}/\partial R|^2$. To see why this comes about, consider two neighbouring annuli of equal mass at radii R, $R+\Delta R$ and with tilts $\boldsymbol{l}$, $\boldsymbol{l}+\Delta\boldsymbol{l}$. Now allow these annuli at fixed radius to use the (R, z) stress, governed by ν_2, to share angular momentum and remove the mutual twist. Having done so, they will both achieve a tilt of $\boldsymbol{l}+\xi\Delta\boldsymbol{l}$, where $0<\xi<1$. However, to achieve this, both annuli have had to dissipate the energy associated with motion perpendicular to the plane whose normal is given by $\boldsymbol{l}+\xi\Delta\boldsymbol{l}$, and so both annuli must move inwards to reachieve centrifugal balance in the radial direction. Thus the second term on the right-hand side corresponds to the inward flow associated with the local untwisting of the twisted disc. We further remark that it is evident from the form of the equation that mass is conserved.

From equations (2.1) and (2.2) we may also derive an equation for the time evolution of the disc tilt. This equation may be written in the form

$$\frac{\partial\boldsymbol{l}}{\partial t}+\left[V_R-\frac{\nu_1\Omega'}{\Omega}-\frac{1}{2}\nu_2\frac{(\Sigma R^3\Omega)'}{\Sigma R^3\Omega}\right]\frac{\partial\boldsymbol{l}}{\partial R} \tag{2.5}$$

$$=\frac{\partial}{\partial R}\left(\frac{1}{2}\nu_2\frac{\partial\boldsymbol{l}}{\partial R}\right)+\frac{1}{2}\nu_2\left|\frac{\partial\boldsymbol{l}}{\partial R}\right|^2\boldsymbol{l}.$$

In this form it is explicitly apparent that the equation conserves $\boldsymbol{l}$ as a unit vector, that is $\boldsymbol{l}\cdot\partial\boldsymbol{l}/\partial t=0$, since $\boldsymbol{l}\cdot\delta\boldsymbol{l}/\partial R=0$.

Equations (2.4) and (2.5) govern the evolution of the disc. However, since $|\boldsymbol{l}|=1$, the equations (2.4) and (2.5) in reality only govern the evolution of three independent scalar quantities. Thus we should be able to replace these two equations by a single equation governing the evolution of a vector quantity. To do this we define $\boldsymbol{L}=\Sigma R^2\Omega\,\boldsymbol{l}$, which is the local angular momentum density in the disc. In other words, the annulus between $R-\frac{1}{2}\Delta R$ and $R+\frac{1}{2}\Delta R$ has total mass $\Delta M=2\pi\Sigma R\Delta R$ and total angular momentum $\Delta\boldsymbol{L}=2\pi\boldsymbol{L}R\Delta R$, to first order in ΔR. The equation governing the evolution of $\boldsymbol{L}$ can be written

$$\frac{\partial\boldsymbol{L}}{\partial t}=\frac{1}{R}\frac{\partial}{\partial R}\left\{\frac{(\partial/\partial R)[\nu_1\Sigma R^3(-\Omega')]}{\Sigma(\partial/\partial R)(R^2\Omega)}\boldsymbol{L}\right\}$$

$$+\frac{1}{R}\frac{\partial}{\partial R}\left[\frac{1}{2}\nu_2 R|\boldsymbol{L}|\frac{\partial\boldsymbol{l}}{\partial R}\right] \tag{2.6}$$

$$+\frac{1}{R}\frac{\partial}{\partial R}\left\{\left[\frac{\frac{1}{2}\nu_2 R^3\Omega|\partial\boldsymbol{l}/\partial R|^2}{(\partial/\partial R)(R^2\Omega)}+\nu_1\left(\frac{R\Omega'}{\Omega}\right)\right]\boldsymbol{L}\right\}.$$

In this form it is evident that the equation conserves angular momentum, and it is also easy to see that for a flat disc ($\partial\boldsymbol{l}/\partial R=0$) the equation reduces to the standard disc evolution equation. From a mathematical point of view, the first two terms on the right-hand side are diffusive, and the last term

on the right-hand side is an advective one. This becomes important when setting up a numerical method for solving the equation (see below).

For reference below, we also give the form of the equations for the case of a disc around a central point mass, M. In this case we have $\Omega \propto R^{-3/2}$ and $\boldsymbol{L}=(GMR)^{1/2}\Sigma\boldsymbol{l}$. Then equation (2.4) becomes

$$\frac{\partial\Sigma}{\partial t}=\frac{3}{R}\frac{\partial}{\partial R}\left[R^{1/2}\frac{\partial}{\partial R}(\nu_1\Sigma R^{1/2})\right]+\frac{1}{R}\frac{\partial}{\partial R}\left[\nu_2\Sigma R^2\left|\frac{\partial\boldsymbol{l}}{\partial R}\right|^2\right], \quad (2.7)$$

and equation (2.6) becomes

$$\begin{aligned}\frac{\partial\boldsymbol{L}}{\partial t}=&\frac{3}{R}\frac{\partial}{\partial R}\left[\frac{R^{1/2}}{\Sigma}\frac{\partial}{\partial R}(\nu_1\Sigma R^{1/2})\boldsymbol{L}\right]\\&+\frac{1}{R}\frac{\partial}{\partial R}\left[\left(\nu_2 R^2\left|\frac{\partial\boldsymbol{l}}{\partial R}\right|^2-\frac{3}{2}\nu_1\right)\boldsymbol{L}\right]\\&+\frac{1}{R}\frac{\partial}{\partial R}\left(\frac{1}{2}\nu_2 R|\boldsymbol{L}|\frac{\partial\boldsymbol{l}}{\partial R}\right),\end{aligned} \quad (2.8)$$

where we note that $|\boldsymbol{L}|=(GM)^{1/2}\Sigma R^{1/2}$, and $\boldsymbol{L}/\Sigma=(GMR)^{1/2}\boldsymbol{l}$.

3 APPLICATIONS – THE NUMERICAL SCHEME

For simplicity, we limit ourselves to the case of a disc orbiting around a central point mass, but note that the application to a general rotation law $\Omega(R)$ is equally straightforward. The applications therefore require numerical solution of equation (2.8). It is important to use a numerical difference scheme which keeps track of conservation of angular momentum as far as is possible, and we briefly describe here how this is done. The method we employ is first-order explicit, using standard differencing from the diffusion term (the first and third terms on the right-hand side of equation 2.8) and the Lelevier method (i.e., upstream differencing) for the advection term (the second term on the right-hand side of equation 2.8) (Potter 1973). We use a simple set of Cartesian (xyz) coordinates and treat each component of equation (2.8) separately.

The independent variable in equation (2.8) is $\boldsymbol{L}(R, t)$, which is evaluated at each such point, and from this we can deduce both $\boldsymbol{l}(R, t)$ and $\Sigma(R, t)$. From these we generate the values of $\boldsymbol{l}$ at the half-grid points on the mesh by simple averaging (and then ensuring the resultant values have $|\boldsymbol{l}|=1$). Then the first term on the right-hand side can be discretized in such a fashion that angular momentum is conserved exactly, provided that we adopt the boundary conditions equivalent to $\partial(\nu_1\Sigma R^{1/2})/\partial R=0$, i.e., zero torque, at the half-grid points just inside each end of the mesh. The other diffusive term (the third term on the right-hand side of equation 2.8) can similarly be written in conservative form. To do this we need to evaluate the quantity $\nu_2\Sigma$ at the half-grid points, which is done by simple averaging, and the quantity $\mathrm{d}\boldsymbol{l}/\mathrm{d}R$ at the half-grid points, which is obtained from $\boldsymbol{l}$ at the whole mesh points by simple differencing. We then also need to impose the boundary condition equivalent to $\partial\boldsymbol{l}/\partial R=0$ again at the half-grid points just inside each end of the mesh. This is equivalent to a free boundary (zero torque) for the disc tilt. For the advective term (the second term on the right-hand side of equation 2.8) we define the advective velocity

$$V_{\mathrm{adv}}=\frac{3}{2}\frac{\nu_1}{R}-\nu_2 R\left|\frac{\partial\boldsymbol{l}}{\partial R}\right|^2 \quad (3.1)$$

at whole grid points and then employ upstream differencing dependent on the sign of V_{adv}. For a flat disc, $V_{\mathrm{adv}}>0$ and the upstream differencing leads to a loss of angular momentum at the outer disc edge. For a steady-state disc this loss is equivalent to a zero radial velocity boundary condition at the outer disc edge. For the applications below, V_{adv} is usually positive everywhere at all times. The exception occurs in the initial configuration of the simple twist (Section 3.1), when for the first few time-steps V_{adv} may change sign in the grid where the initial twist is implemented. A change of sign of V_{adv} in a mid-grid can also lead to non-conservation of angular momentum, but this is usually small and brief.

Thus far we have set up a difference scheme which tracks angular momentum flux to machine accuracy and conserves mass to the order of the scheme. The scheme on its own leads naturally to certain boundary conditions which may not correspond to the relevant physics in a given application. At both boundaries the scheme ensures that no torque is provided in either the azimuthal or the tilt direction. At the outer boundary, however, there is an outflow of angular momentum (and therefore mass) at rate V_{adv}. Thus, to model a completely free outer boundary, it is necessary to choose an outer mesh boundary well beyond where most of the disc mass lies. For the applications below, we are interested in the tilt behaviour in the inner regions of an otherwise steady disc, and thus the freely advecting outer boundary is adequate for us. At the inner boundary there is no torque, and so no loss of angular momentum and no net inflow of mass. The usual numerical models of time-dependent accretion discs take $\Sigma=0$ at the inner edge, which assumes no viscous torque there and thus leads to advection of matter inwards (i.e., accretion) – see for example Pringle, Verbunt & Wade (1986). In order to produce an accreting, but torque-free, inner boundary, we set up a sink of material there. In effect, we add a term to the right-hand side of equation (2.8) of the form

$$\frac{\partial\boldsymbol{L}}{\partial t}=-\boldsymbol{L}f(R)/t_{\mathrm{sink}}, \quad (3.2)$$

where $f(R)$ is a dimensionless function which is strongly peaked close to the inner edge, and t_{sink} is an adjustable timescale which is chosen to be suitably small to give rise to an approximation of the usual $\Sigma=0$ inner boundary condition. In similar fashion, in order to set up a steady-state disc it is convenient to add matter close to the outer edge at a well-defined rate spread over a few grid-zones.

4 APPLICATIONS – THE RESULTS

4.1 Steady-state disc

We work initially with 41 grid points spaced logarithmically between $R_{\mathrm{in}}=1$ and $R_{\mathrm{out}}=40$. We add matter to the grid at a rate $\dot{M}_{\mathrm{in}}=1$ in the range $R=29$ to 37, with a spatial distribu-

tion (suitably discretized) in the form of a cosine bell (covering three zones). In order to set up a twisted disc, we add the matter in such a way that the angular momentum is as required. We adopt an input angular momentum such that the input matter forms a ring with angle of inclination $i=0.5$ rad to the z-axis, and such that the azimuth of the ascending node is at $\omega=0$ (i.e., lying along the x-axis). For simplicity, we choose the viscosities to be $\nu_1=1$ and $\nu_2=1$. This is roughly equivalent to choosing units of time such that the viscous time-scale near the inner edge is unity.

As an initial condition, we take the surface density to be Σ_{SS}, which corresponds to a steady-state disc with inner accreting ($\Sigma=0$) radius R_{in}, outer radius R_{out} at which $V_R=0$, and radius R_{add} at which matter is added in the form of a delta function. For $\nu_1=1$ and $\dot{M}=1$, this has the form

$$\Sigma_{SS}=\begin{cases}(R^{1/2}-R_{in}^{1/2})/3\pi R^{1/2}, & R_{in}<R<R_{add},\\ (R_{add}^{1/2}-R_{in}^{1/2})/3\pi R^{1/2}, & R_{add}<R<R_{out}.\end{cases} \quad (4.1.1)$$

This is plotted in Fig. 1. We take the initial angular momentum direction to be given everywhere by $i=0.5$ rad, $\omega=0$.

For mass loss at the inner edge, we remove matter on a time-scale $t_{sink}=0.1$ and over a spatial distribution given by a cosine bell extending from $R=R_{in}=1$ out to $R=1.4$ (covering three zones). The time-step is chosen to be short enough to easily satisfy the usual numerical stability criteria (Potter 1973). For most of the time, it is set by the diffusion time-scale across the innermost zone and corresponds to $\Delta t=5\times10^{-4}$.

We then run the scheme until a steady state is established, which we judge as having happened when the accretion rate at the inner edge tends to a constant value. The viscous time-scale for such a disc is $t_\nu\sim R_{out}^2/\nu\sim1600$, and indeed we find that a time-scale of $t=2000$ is adequate to achieve a steady state. The steady-state surface density distribution is also shown in Fig. 1. Note that the discrepancy between the analytic and numerical results comes about because the boundary conditions are not exactly the same. In particular, in the numerical scheme we do not have $\Sigma=0$ at $R=R_{in}$ (although we could approach this by decreasing t_{sink}), and, more importantly, in the numerical scheme we can lose angular momentum at the outer edge (to mimic $V_R=0$) only by losing mass there. Thus not all the matter added at R_{add} is accreted at the inner edge R_{in}. We find that in this case 78 per cent of the added matter is accreted at $R=R_{in}$.

4.2 Evolution of a simple twist

To study the evolution of a simple twist in an otherwise steady accretion disc, we generate an initial state by taking the steady-state tilted disc (with $i=0.5$ rad, $\omega=0$) and flatten the inner portion of it into the xy-plane. To be specific, we take the same surface density distribution as before, but rotate the inner parts, $1\le R\le10$, to ensure $i=0$ there. In order to ensure numerical stability and accuracy, we then smooth the abrupt jump in inclination at $R=10$ over five zones, using (roughly from $R=8.2$ to 12.2) a sinusoidal profile. The initial inclination profile is shown in Fig. 2.

We then evolve the disc as before using the same boundary conditions as in Section 4.1. Thus the outer disc acts as a large reservoir of tilt and gradually overwhelms the flattened inner region. The evolution of the inclination profile with time is also shown in Fig. 2. Note that the viscous evolution time-scale at $R=10$ is of order $t_\nu\sim R^2/\nu\sim100$, and this is indeed roughly the time-scale on which the twist in the inner

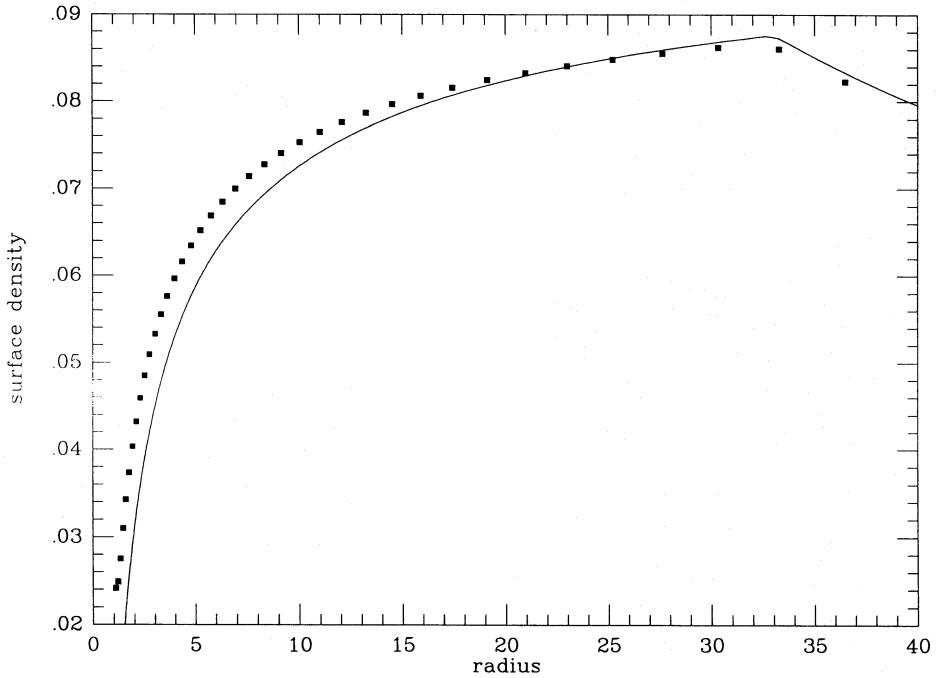

Figure 1. The surface density distribution for a steady-state disc with $\nu_1=1$. The solid line is the distribution obtained analytically for a disc gaining material at $R=37$, with a $V_R=0$ boundary condition at $R=40$ and an accreting ($\Sigma=0$) boundary condition at $R=1$. The points represent the approximation to this solution obtained with the numerical method described in the text. As discussed in the text, the main difference comes about because of the outer boundary condition.

regions is smoothed out. Note too that the line of nodes remains unchanged throughout. As we remarked in Section 2, the region in which the straightening out of the disc twist occurs also experiences a net inflow of material because the combining of different angular momenta results in a lessening of centrifugal support in the radial direction. This can be seen in the evolution of the surface density with time (Fig. 3). This leads in this case to a slight (2–3 per cent) increase in the inner accretion rate, which peaks at a time of around $t=7.5$. The inner accretion rate returns to normal at a time of about $t=20$ and then, to compensate, dips below average until around $t=200$, after which it returns to the previous steady-state value.

4.3 Forced precession at the inner edge: the Bardeen–Petterson effect

The situation in which the individual disc elements undergo forced precession is relatively easy to model using the current formulation. If each disc annulus precesses at a rate $\boldsymbol{\Omega}_{\rm p}(R)$, then we add a term to the right-hand side of equation (2.6) (or, equivalently, equation 2.8) of the form

$$\frac{\partial \boldsymbol{L}}{\partial t} = \boldsymbol{\Omega}_{\rm p} \times \boldsymbol{L}. \tag{4.3.1}$$

This is implemented numerically in a straightforward first-order and explicit manner.

As an illustration, we consider the case of an accretion disc in orbit around a misaligned Kerr black hole. We consider the effect of Lense-Thirring precession on the inner disc. Bardeen & Petterson (1975) pointed out that the combined effect of the precession and viscosity should be to align the rotation of the inner disc with the spin axis of the hole. Using the above equations, but linearized for a slightly tilted disc, and for a steady state, Kumar & Pringle (1985) showed that the alignment of disc and hole does take place, but that the twisting occurs over a large range of radii. For this reason, we use an extended numerical grid of 101 points extending from $R=1$ to 1.012×10^4, which ensures that the innermost 41 grid points coincide with the previous grid discussed above.

We add material as before over a range of radii from $R=4000$ to 6000, covering three zones. As in Section 4.1, we set up an initial disc which corresponds to the analytic solution given by equation (4.1.1), with a tilt angle of $i=0.5$ rad. We then evolve the disc for a time of 1000 in order to allow the inner parts in which we are interested to settle into the numerical equilibrium state.

We then continue the evolution, but apply forced precession in the inner parts. Following Kumar & Pringle (1985), we take the precession to be of the form

$$\boldsymbol{\Omega}_{\rm p} = (0, 0, \omega_{\rm p} R^{-3}), \tag{4.3.2}$$

where $\omega_{\rm p}$ corresponds roughly to the precession time-scale at the inner disc edge expressed in units of the radial viscous time-scale there. The canonical measurement of the Bardeen–Petterson radius, $R_{\rm BP}$, which is, loosely speaking, the radius inside which the disc aligns with the spin of the black hole, is given by writing $|\boldsymbol{\Omega}_{\rm p}|\, t_R \sim 1$, where $t_R \sim R/|V_R|$ is the radial drift time-scale. Using equation (4.1.1) to give

$$t_R = \frac{2}{3} R^2 \left(1 - \frac{R_{\rm in}^{1/2}}{R^{1/2}}\right), \tag{4.3.3}$$

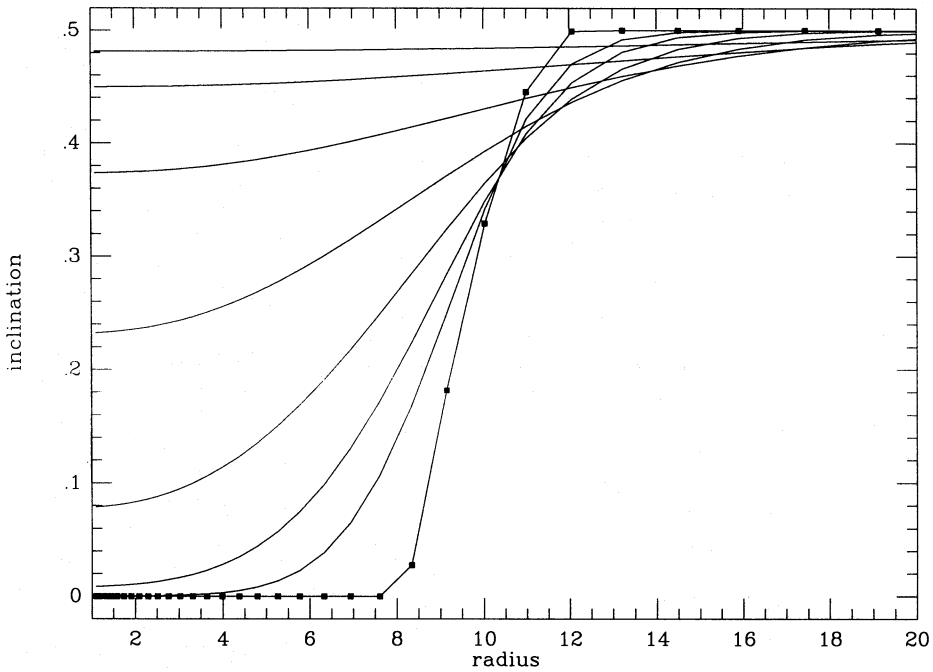

Figure 2. The evolution of a twist in a 'steady' disc. The disc inclination (in radians) is plotted against radius as a function of time. The initial disc ($t=0$) is as shown in Fig. 1 except that a twist has been introduced inside $R=10$. The $t=0$ inclination distribution is marked by the solid squares. As time proceeds the twist slowly evolves until the disc is eventually flat again at inclination $i=0.5$ rad. The curves plotted correspond to times $t=0$, 2.5, 5, 10, 20, 40, 80 and 160.

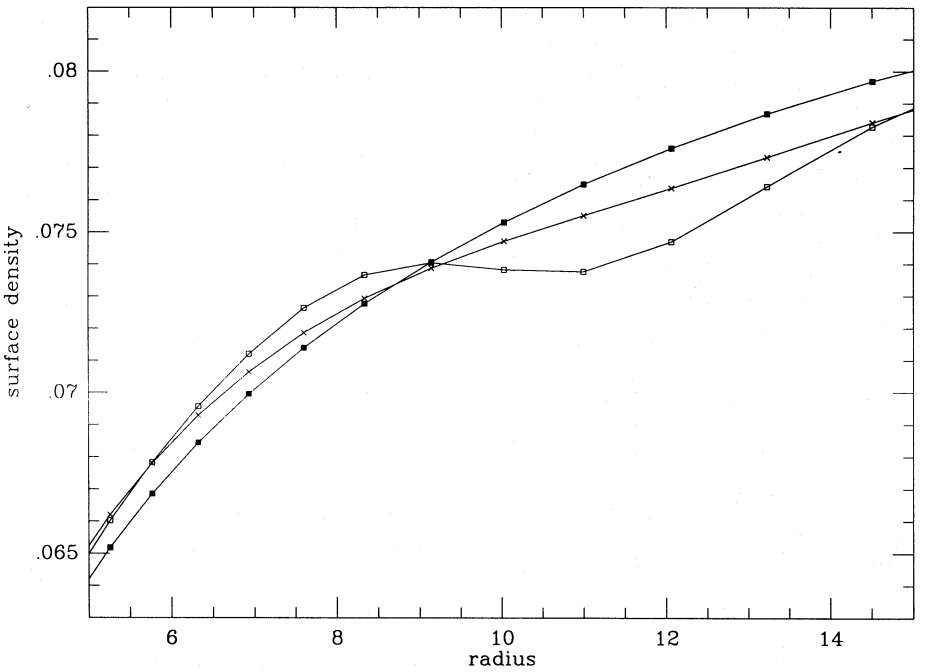

Figure 3. The initial variations in the surface density distribution are shown for the case of evolution of twist shown in Fig. 2. The solid squares are at time $t=0$ and correspond to the same solution as Fig. 1. The open squares are at time $t=2.5$ and the crosses at $t=10$.

we obtain R_{BP} as the solution of

$$R_{BP}\left[1-\left(\frac{R_{in}}{R_{BP}}\right)^{1/2}\right]^{-1}=\frac{2\omega_p}{3}. \qquad (4.3.4)$$

We shall choose $\omega_p=20$, which gives $R_{BP}\approx 9$. We note that R_{BP} is defined in terms of the radial drift time-scale (e.g. Rees 1976), and so depends only on the radial shear viscosity ν_1. The time-scale on which the precession takes effect at R_{BP} is given by

$$t_R(R_{BP})\approx R_{BP}^3\Omega_p^{-1}\approx 36, \qquad (4.3.5)$$

and also corresponds to the time-scale on which a steady-state disc twist might be set up (cf. Kumar & Pringle 1985).

In Fig. 4 we show the evolution of the inclination in the inner disc as a function of time after the precession has tuned on, for the case in which $\nu_1=\nu_2=1$. Although a steady state is never achieved, it is evident that the twist evolution is slowing down rapidly, and that after a time of 200 we are approaching a stage where the outer twist has been reduced by a factor of 2 within a radius of order R_{BP}. As noted by Kumar & Pringle (1985), the range in radii over which the disc tilt differs significantly from its original (outer) value and from zero is very large. For this reason, the time-scale for setting up a disc with a steady tilt due to the Bardeen–Petterson effect is much longer than simply the flow time-scale or the precession time-scale at the nominal Bardeen–Petterson radius.

In Fig. 5 we show the same calculation, but this time with $\nu_1=1$, $\nu_2=0.1$. It is evident that the flattening of the disc in the inner regions now occurs on a longer time-scale, but not a factor of 10 longer, indicating that the effect of alignment is due to a combination between the two viscosities. By the time $t=2000$, the two solutions are more or less the same, at least out to a radius of order R_{BP}.

5 DISCUSSION

The main purpose of this paper has been to demonstrate a simple numerical scheme describing the evolution of a twisted accretion disc subject to external torques. The scheme is set up so that it identically conserves angular momentum, when appropriate. The scheme is general in that it may be used with discs with any tilt angle.

The main uncertainties in the scheme regarding the transport of angular momentum within the disc are contained within the two 'viscosities', ν_1 and ν_2. If we consider a particular radius in the disc, local cylindrical coordinates (R, θ, z) with the disc lying in the $z=0$ plane, then ν_1 corresponds to the (R, θ) shear whereas ν_2 corresponds to the (R, z) shear. These are physically distinct quantities and there is no reason, except for molecular viscosity in Newtonian fluids, why they should be the same. For example, if angular momentum transport is effected by fluid turbulence within the disc, then it seems likely that the strong radial shear in the disc would render such turbulence anisotropic, and thus imply different effective viscosities for different components of shear. Again, if angular momentum transport is effected by magnetic stresses (in effect magnetohydrodynamic turbulence), then since the (R, θ) shear has a secular effect on neighbouring fluid elements, whereas the (R, z) shear has an oscillatory one (with frequency Ω), the angular momentum transport process in each case is quite distinct. The (R, z) shear is propagated by emission of Alfvén waves, whereas the (R, θ) shear effects a continuous stretching of the magnetic field. In the calculations here we have taken both ν_1 and ν_2 as constants, but in general they are likely to be functions of local variables.

Although we have applied the numerical scheme solely to Keplerian accretion discs, as we remarked above, it can be applied equally well to any physical rotation law, $\Omega(R)$, that

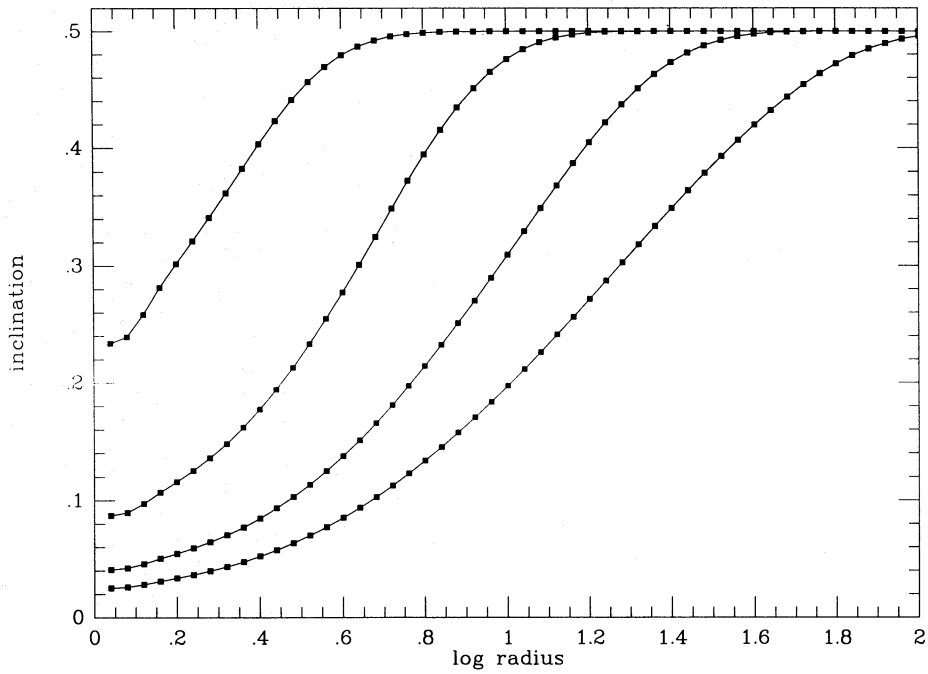

Figure 4. Disc inclination, i, is plotted against radius for various values of time t. At $t=0$ the disc is in a steady state with $i=0.5$ rad. At that stage the inner parts of the disc are forced to precess at a rate $\Omega_p \propto R^{-3}$ about the $i=0$ axis. As the disc evolves, more and more of the disc becomes aligned with $i=0$. The plots shown here are at times $t=2$, 20, 200 and 2000. This plot is for $\nu_1=\nu_2=1$.

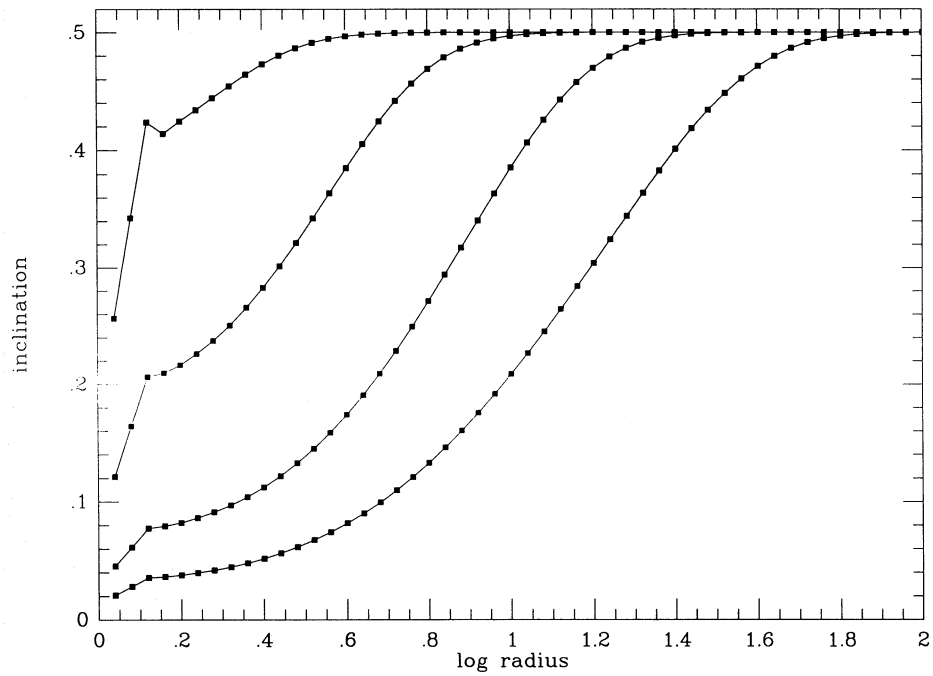

Figure 5. As for Fig. 4 but with $\nu_1=1$ and $\nu_2=0.1$.

is, one which satisfies $\mathrm{d}\Omega/\mathrm{d}R<0$ and $\mathrm{d}(R^2\Omega)/\mathrm{d}R>0$. In particular, it is straightforward to model disc evolution in an axisymmetric potential, as long as it is adequate to describe the motion of an orbiting ring in terms of Ω which is solely a function of radius, R, coupled with a precession rate Ω_p which can be a function both of radius R and of local disc inclination $i(R)$. It would be an interesting exercise to see how well such a simple description can model the dynamical particle simulations of misaligned gaseous rings, such as those carried out by Varnas (1990) and Katz & Rix (1992). A major consideration here would be estimation of the effective viscosities ν_1 and ν_2 in the particle schemes. We also note that the present scheme can be straightforwardly adapted to include the effects of mutual self-gravity on the

disc elements (cf. Ostriker & Binney 1989; Kuijken 1991), at least as far as the twist is concerned. Of course, if the disc mass contributes substantially to the potential in which the disc orbits, then one has to allow for the fact that Ω is a function of time (cf. Lin & Pringle 1990).

ACKNOWLEDGMENT

I thank Dr S. H. Lubow for stimulating and valuable discussions.

REFERENCES

Athanassoula E., Bosma A., 1985, ARA&A, 23, 147
Bardeen J. M., Petterson J. A., 1975, ApJ, 195, L65
Borderies N., Goldreich P., Tremaine S., 1984, ApJ, 284, 429
Coleman C. S., Kumar, S., 1992, Proc. Astron. Soc. Aust., in press
Gunn J. E., 1979, in Hazard C., Mitton S., eds, Active Galactic Nuclei. Cambridge University Press, Cambridge, p. 213
Habe A., Ikeuchi S., 1985, ApJ, 289, 540
Hatchett S. P., Begelman M. C., Sarazin C. L., 1981, ApJ, 247, 677
Kahn F. D., Woltjer L., 1959, ApJ, 130, 705
Katz N., Rix H. W., 1992, ApJ, 389, L55
Kuijken K., 1991, ApJ, 376, 467
Kumar, S., Pringle J. E., 1985, MNRAS, 213, 435
Lin D. N. C., Pringle J. E., 1990, ApJ, 358, 415
Lubow S. H., 1992, ApJ, in press
Ostriker E. C., Binney J. J., 1989, MNRAS, 237, 785
Papaloizou J. C. B., Pringle J. E., 1983, MNRAS, 202, 1181
Petterson J. A., 1977, ApJ, 214, 550
Petterson J. A., 1978, ApJ, 226, 253
Potter D., 1973, Computational Physics. J. Wiley & Sons, New York
Pringle J. E., 1981, ARA&A, 19, 137
Pringle J. E., Verbunt F., Wade R. A., 1986, MNRAS, 221, 169
Rees M. J., 1976, in Eggleton P., Mitton S., Whelan J., eds, Structure and Evolution of Close Binary Stars. Reidel, Dordrecht, p. 225
Steiman-Cameron T. Y., Durisen R. H., 1988, ApJ, 325, 26
Tubbs A. D., 1980, ApJ, 241, 969
Varnas S. R., 1986, Proc. Astron. Soc. Aust., 6, 458
Varnas S. R., 1990, MNRAS, 247, 674